Meta-Substituted Benzofused Macrocyclic Lactams as Zinc Metalloprotease Inhibitors

Gary M. Ksander,* Reynalda de Jesus, Andrew Yuan, Raj D. Ghai, Colin McMartin,† and Regine Bohacek‡

Research Department, Pharmaceuticals Division, CIBA-GEIGY Corporation, 556 Morris Avenue, Summit, New Jersey 07901

Received August 8, 1996⊗

The design, synthesis, and biochemical profile of meta-substituted benzofused macrocyclic lactams are described. The meta-substituted benzofused macrocyclic lactams were designed to have a degree of flexibility allowing the amide bond to occupy two completely different conformations while maintaining sufficient rigidity to allow for strong interaction between enzyme and inhibitor. Using TFIT, a novel molecular superimposition program, it was shown that the meta analogs could be readily superimposed onto our ACE inhibitor template whereas no low-energy superimpositions of the ortho-substituted macrocycles could be found. The macrocycles were prepared by tethering aldehyde **1** derived from *S*-glutamic acid or *S*-aspartic acid to a meta-substituted phosphonium bromide **2**. Homologation to a monocarboxylic acid methyl ester malonate followed by deprotection and cyclization gave the macrocyclic frame. Further manipulation gave the desired compounds. Unlike the ortho-substituted benzofused macrocyclic lactams described in the previous paper which are selective NEP inhibitors, the meta-substituted compounds are dual inhibitors of both NEP and ACE. The most potent member of this new series, compound **16a**, inhibited both enzymes with an $IC_{50} = 8$ nM in NEP and 4 nM in ACE.

Introduction

There has been considerable interest over the past few years in dual angiotensin converting enzyme (ACE) and neutral endopeptidase (NEP) inhibitors. Simultaneous blockade of angiotensin II production and increasing atrial naturetic peptide levels should have a beneficial effect in the treatment of hypertension and other cardiovascular and renal diseases. A number of investigators have studied the structural similarities of the active site of these two enzymes and the incorporation of both NEP and ACE inhibitory activities within a single chemical entity.[1a−1g] The previous paper describes the use of an active site model to predict NEP activity based on the crystal structures of the bacterial zinc metalloprotease thermolysin. The macrocyclic lactams described in the previous paper were either inactive or very weak inhibitors of ACE. However, they exhibited potent NEP and/or thermolysin inhibitory activity. Using the previously described model of NEP and a template compiled from existing ACE inhibitors, we set out to investigate if modifications could be made that would give these compounds the flexibility to bind to both NEP and ACE while maintaining a degree of rigidity that allows for a strong interaction between enzyme and inhibitor. In this paper we describe a simple structural change to the previously described macrocycles which allows these selective NEP inhibitors to inhibit both enzymes, NEP and ACE.

Molecular Modeling

Construction of an ACE Inhibitor Composite Template. An ACE inhibitor template had previously been constructed using four potent conformationally restricted inhibitors. (See compounds **A**−**D** shown in Figure 2.[2]) The procedure will be briefly summarized here. A zinc atom was connected to the zinc-ligating group of each inhibitor using geometrical parameters obtained from X-ray crystal diffraction data both of small molecules[3] and enzyme/inhibitor complexes. A new computer program, TFIND,[4a,b] was then used to superimpose the four inhibitors so that chemically equivalent atoms of one molecule occupied the same volume as the corresponding atoms of the other molecules. This program combines a thorough search of low-energy conformations of each molecule with simultaneous superimposition by adding a superimposition force field to the potential function. In this way, the internal energy of the molecule and its superimposition energy are cominimized. For more details, see the Experimental Section. TFIND found three different good superimpositions of low-energy conformations of these four molecules.

Three-dimensional templates for ACE inhibitors have previously been developed by other researchers using a variety of different methods.[3,5,6] All of these templates as well as the superimpositions found by TFIND agree as to the conformations the inhibitors adopt between the P_1' side chain and the C-terminal carboxylic acid. However, there is little agreement concerning the bioactive conformation of the remaining portions of the inhibitors.

To develop a hypothesis concerning the conformation adopted by ACE inhibitors between the catalytic zinc and the P_1' carbonyl, we turned to structural data. Examination of the crystal structures of known zinc metallo exo- and endo-protease/inhibitor complexes revealed strong conformational similarities of this region for all of the inhibitors.

Although the crystal structure for ACE has not been determined, similarity in conserved sequence motifs and mutagenesis experiments suggest that the region of the two active sites of ACE close to the zinc may resemble that found in other zinc metalloproteases. ACE displays the characteristic HEXXH[7] motif found in thermolysin,[8] NEP,[9,10] and the metzincins.[11,12] From the crystal structures of thermolysin[13] and members of four sub-

* Author to whom correspondence should be addressed.
† Current address: Thistlesoft, Lindsley Dr., Suite 302, Morris Township, NJ 07960.
‡ Current address: Ariad Pharmaceutical, Inc., 26 Landsdowne St., Cambridge, MA 02139.
⊗ Abstract published in *Advance ACS Abstracts,* January 15, 1997.

S0022-2623(96)00583-3 CCC: $14.00

families of the metzincins,[14−24] it is known that the two histidines bind to the catalytic zinc. The glutamic acid adopts the same relative position in all of these enzymes and has been proposed to be essential for catalysis.[13] Mutagenesis experiments suggest that these residues have the same function in NEP.[25,26] A second conserved sequence, NEXIXD, is shared by ACE, thermolysin, and NEP. Again, mutagenesis experiments with ACE[27] and NEP[28] indicate that, as in thermolysin, the glutamic acid is the third zinc binding residue.

We, therefore, made the assumption that the regions close to the zinc in ACE are likely to be similar to those found in other zinc metalloproteases and that when inhibitors bind to ACE, they will also adopt the conformation near zinc found in the crystal structures of other metalloprotease inhibitor complexes. Only one of the templates generated by the TFIND program displayed this geometry and was, therefore, proposed as a pharmacophore for ACE. This ACE inhibitor template has been extensively tested and was able to distinguish between active and inactive ACE and dual ACE/NEP inhibitors from a number of different laboratories.[2]

The first set of macrocycles described in this work has a phenyl ring in the P_1' position. To provide more information concerning the allowed volume in the S_1' subsite of ACE, we added an additional potent, conformationally restricted inhibitor, **E**,[29] to the template. Figure 3 shows the resulting ACE inhibitor template used in the present work.

Once the template was constructed, the TFIT program was used to determine if low-energy conformations could be found for each macrocycle that would allow chemically similar atoms of the macrocycle to be superimposed onto the corresponding atoms of the template. Like TFIND, the TFIT program also uses the superimposition force field. However, when using TFIT, the template is held rigid and only the test molecule is subjected to conformational searching and cominimization of internal and superimposition energy. (Additional details are given in the Experimental Section.)

Besides the superimposed structures, the output of the TFIT program reports two parameters: the ligand strain energy which approximates the cost in energy required for a test compound to adopt the superimposed conformation and the superimposition energy which is a measure of how closely atoms of the test compound can fit on chemically similar atoms of the template.

The starting structures for the template fitting were either obtained directly from the NEP studies described in the preceding paper or constructed using the procedures also described in that paper. Next, using the MACROMODEL[30] molecular modeling program, a zinc atom was added to the sulfur of each macrocycle with a zinc−sulfur bond length of 2.3 Å and a zinc−sulfur−carbon angle of 100°. These parameters are based on small molecule crystal structures of relevant compounds from Cambridge Structural Database given by Hausin and Codding.[3] Then each macrocycle was subjected to template fitting with 1000 search cycles. To provide an additional measure of how well each structure fit onto the template, the volume of the template plus the superimposed macrocycle was determined using MACROMODEL.

Chemistry

Condensation of aldehyde **1** derived from L-glutamic acid with the aryl phosphonium bromide **2** under standard Wittig conditions gave the olefin **3** in good yield (Scheme 1). Metal halogen exchange, using BuLi with aryl bromide **3**, followed by DMF condensation gave the benzaldehyde derivative **4**. Homologation with the mixed benzyl methyl malonate ester followed by hydrogenation in one step reduced the two double bonds and unmasked one of the carboxylic acid groups to give compound **6**. Cyclization with EDCI to the macrocyclic lactam **8**, after deprotection of the amino alcohol, was accomplished in low yield under dilute reaction conditions. Oxidation of the macrocyclic alcohol **8** with sodium periodate/ruthenium trichloride followed by saponification with sodium hydroxide gave the diacid **10**. The exocyclic double bond was introduced by reaction of the carboxylic acid/amide with paraformaldehyde and piperidine followed by decarboxylative elimination. Addition of thioacetic acid to the enone **11** and reesterification with diazomethane gave a mixture of two diastereomers **13a,b**. These diastereomers could be readily separated by flash chromatography. The diastereomers were easily distinguishable in the NMR by the position of the NH and the NHC*H*CO_2CH_3 methine protons. However, the relative stereochemistry (cis and trans) could not be assigned by NMR studies alone, due to the flexibility of the macrocyclic ring.

The relative and thus the absolute stereochemical assignment is based on the synthetic procedures (starting from L-glutamic acid) and the X-ray of **13b**, Figure 1. The X-ray of the 14-membered ring macrocycle, **13b**, clearly shows a trans relationship between the carboxy and methylenethiolacetyl groups. Since the synthetic sequence begins with L-glutamic acid, **13b** can be assigned the *R*(methylene thiol acetyl),*S*(carboxy) configuration. Therefore, **13a** should be the *S,S* diastereomer. The stereochemistry of the 13-membered ring diastereomers **15a**,**b** were assigned by comparing the chemical shift of the NHC*H*CO_2CH_3 methine proton in the ^{1}HNMR and polarity relationship of the *S,S* diastereomers **13a** and **15a** to the *R,S* diastereomers **13b** and **15b** on silica gel plates. The *S,S* diastereomers were more polar on silica gel thin layer plates (EtOAc/Hex, 1:4), displayed a downfield shift in the proton NMR for the NH amide protons (5.87 and 5.60 ppm vs 5.65 and 5.40 ppm, respectively) and an upfield shift for the NHC*H*CO_2CH_3 methine proton (4.28 and 4.02 ppm vs 4.47 and 4.50 ppm, respectively). This relationship between polarity and proton NMR shifts from the assigned diastereomers was also consistent within the ortho-substituted macrocyclic lactam series outlined in the preceding paper. Therefore the stereochemical assignments were made on the basis of chemical synthesis, X-ray analysis, R_f (silica gel), and proton NMR shifts. In addition the stereochemical assignment is also supported by the corresponding chemical shifts determined for the 10-membered ring macrocycle,[1c] the cysteine-containing macrocycle,[1n] and the ortho-substituted benzofused macrocycles described in the previous paper.

Simultaneous saponification of the *S*-acetyl and methyl ester in **13a,b** gave the desired dual inhibitors **14a** and **14b**. Compounds **16a** and **16b** were prepared in an analogous fashion.

Results and Discussion

The ortho-substituted benzofused macrocycles (11-, 12-, and 13-membered rings) are potent inhibitors of

Scheme 1[a]

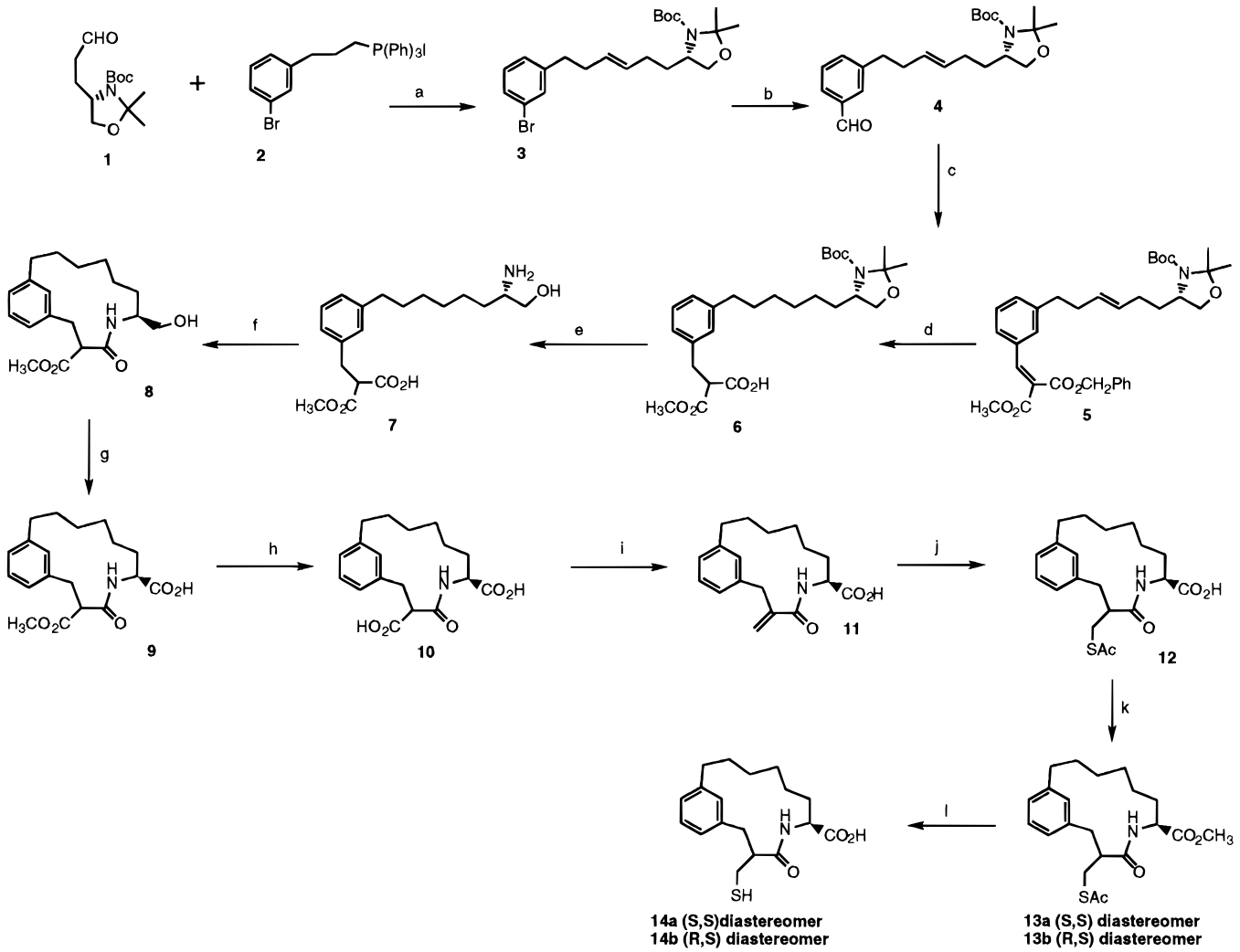

[a] (a) *t*-BuOK; (b) BuLi, DMF; (c) benzyl methyl malonate, piperidine, benzoic acid; (d) H_2/Pd−C; (e) HCl; (f) EDCl, HOBT; (g) $NaIO_4$, $RuCl_3$; (h) NaOH; (i) paraformaldehyde, piperidine; (j) thiolacetic acid; (k) diazomethane, separate diastereomers; (l) LiOH.

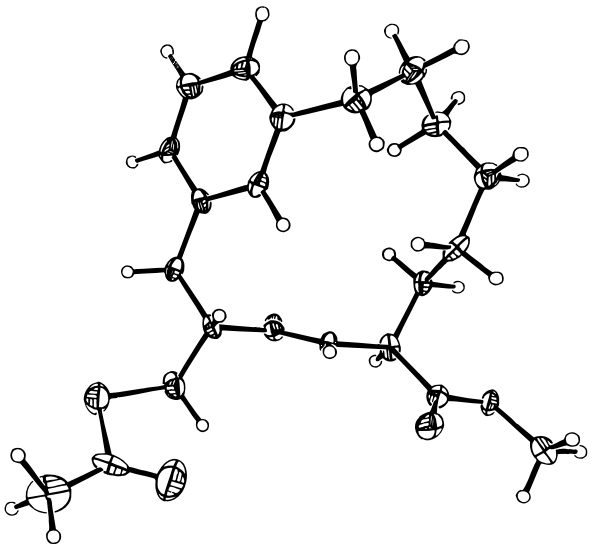

Figure 1. X-ray crystal structure showing absolute configuration of compound **13b**.

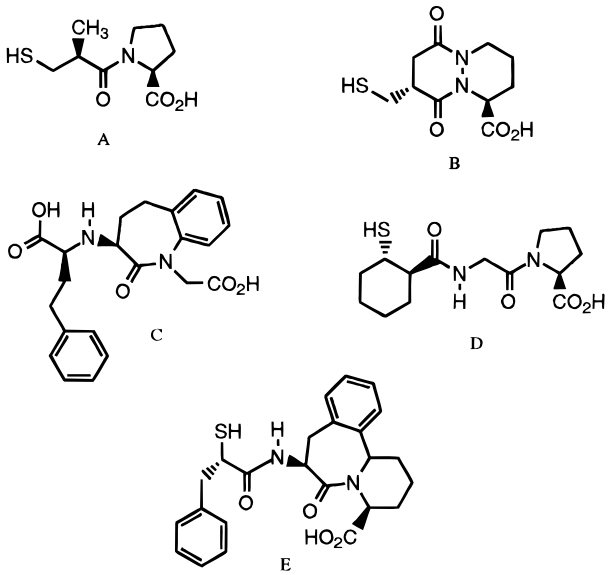

Figure 2. Structures used to generate ACE template.

NEP (Table 1). However they lack significant ACE inhibitory activity. Therefore, these compounds were matched to an ACE molecular model template fitting program to determine if steric fit, hydrogen bonding, or thiol zinc chelation might play a role in the inactivity of these compounds.

On the basis of the structural data from five potent ACE inhibitors a template was constructed to define an active site that would encompass these large molecules. The macrocycles considered here possess considerable flexibility. However, when the thiol, amide, and carboxylic acid moeities are selectively fixed in positions

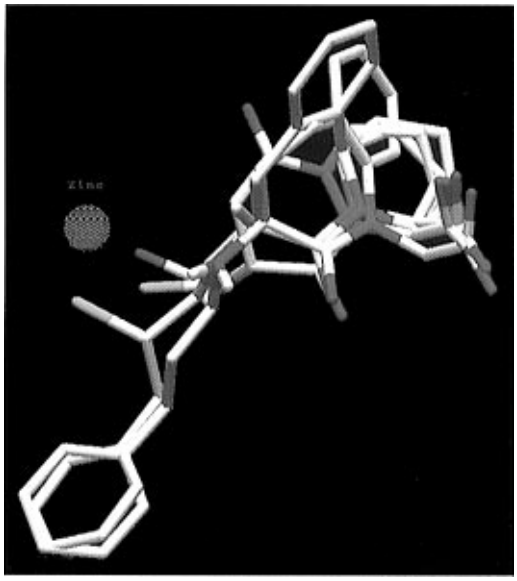

Figure 3. Molecular model of the ACE template.

Table 1. *In Vitro* NEP, ACE, and Thermolysin Inhibition of P_1' Ortho-Substituted Benzofused Macrocyclic Lactams

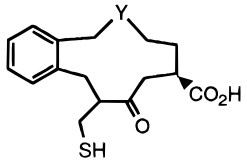

Y = $(CH_2)_n$

			IC_{50} (nM)		
compd	ring size	stereochem	NEP	ACE	TL
17a	11	*S*	0.9	>10000	68
17b	11	*R*	7	>10000	2300
18a	12	*S*	3	8000	600
18b	12	*R*	4	2000	4000
19a	13	*S*	27	>10000	1800
19b	13	*R*	224	>10000	41000

required by the template, the conformation of the carbon backbone becomes less flexible. In some cases a particular high-energy conformation can adopt positions required for good binding to ACE.

Six P_1' ortho-substituted benzofuzed macrocycles varying in ring size from 11 to 13 bonds were compared to an ACE template using the molecular superposition program, TFIT. This program is designed to identify low-energy conformations of the macrocycle which allows the best superimposition of chemically equivalent atoms of the macrocycle onto those of the ACE inhibitor template. The program was biased to retain only those conformations of the macrocycles in which the zinc, the amide carbonyl, and the carboxylic acid lie close to the corresponding atoms of the template. For example, the superimposition of the 13-membered macrocycle **19a** onto the ACE template generated by the program is shown in Figure 4. The energy requirements necessary to obtain the best fit are summarized in Table 4.

None of the P_1' ortho-substituted macrocycles fit well onto the template. This finding is in agreement with the weak ACE inhibitory activity obtained for these compounds. For the four diastereomers of the 11- and 12-membered rings (**17**, **18**), the poor activity can be explained by the high strain energy imposed upon the molecule to acquire the superimposition. However, for **19a** the (*S*,*S*)-13-membered ring diastereomer, a reasonable superimposition of the functional face of the

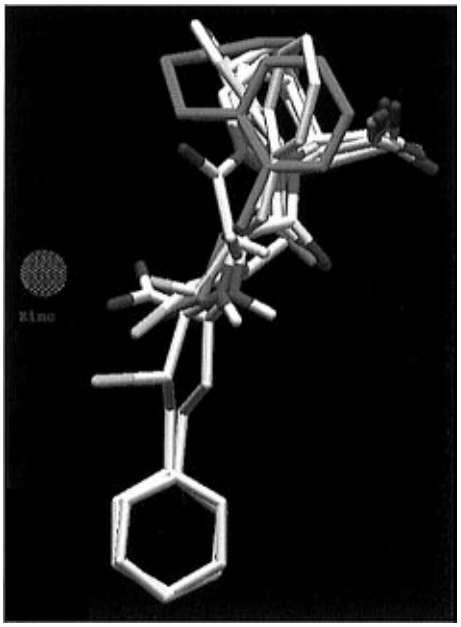

Figure 4. Thirteen-membered ring P_1'(S,S) ortho-substituted benzofused macrocyclic lactam **19a** superimposed on the ACE template. Does not fit well on the template which is consistent with experimental results.

Table 2. *In Vitro* NEP, ACE, and Thermolysin Inhibition of P_2' Ortho-Substituted Benzofused Macrocyclic Lactams

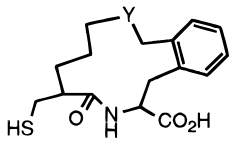

Y = $(CH_2)_n$

			IC_{50} (nM)		
compd	ring size	stereochem	NEP	ACE	TL
20	12	*RS*,*SR* (trans)	99	6000	49000
21a	13	*SS*,*RR* (cis)	67	725	40000
21b	13	*RS*,*SR* (trans)	136	470	16000
22a	14	*SS*,*RR* (cis)	900	NT	NT
22b	14	*RS*,*SR* (trans)	>10000	>10000	60000

molecule is observed with a very low strain energy. At this time, an explanation defining the limitations of the template model/superimposition is worth noting. In this superimposition, three methylene atoms protrude into a space directly behind the template, Figure 4, so that the rest of the macrocycle can match the corresponding template atoms. Without the actual structure of the enzyme/inhibitor complex, it is impossible to accurately identify those regions of the binding site inaccessible to the inhibitor. We assume that if a good overlap occurs between a test molecule and the atoms of the template and if the test molecule is in a low-energy conformation, then good enzyme−inhibitor interactions and high binding affinities should be observed. If, however, atoms of the test molecule lie outside the template in an unmapped area, then the binding interactions between the test molecule and the enzyme cannot be accurately predicted. To explain the poor ACE inhibition of **19a**, however, we must assume that the protruding methylene atoms are positioned in an area forbidden to ligand atoms.

The *in vitro* data for macrocycles with a $P2^1$ ortho-substituted benzofused ring are tabulated in Table 2. Visual inspection of the template modeling with a $P2^1$ benzofused macrocycle, **21a** (Figure 5), resulted in good overlap along the functional side of the template and

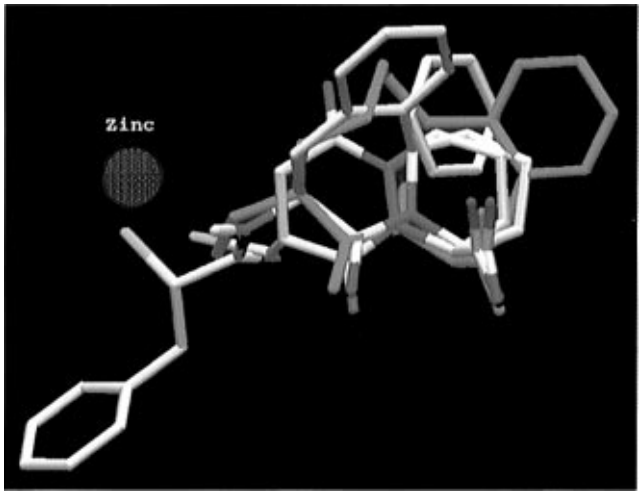

Figure 5. Thirteen-membered ring P_2'(racemic cis) ortho-substituted benzofusedmacrocyclic lactam **21a** superimposed on the ACE template.

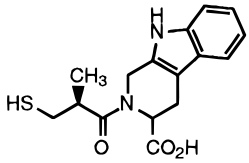

Figure 6. Compound **23**.

good containment within the volume defined by the lipophilic backbone except for the aromatic ring at the $P2^1$ pocket.

The ACE inhibitory activity of **21a** is a modest IC_{50} = 725 nM. Interestingly, we searched our database for compounds that might occupy the same spatial arrangement seen by the protruding aromatic ring at the $P2^1$ site. We found a captopril analog **23,** Figure 6, which models similarly as **21a** and inhibits ACE with an IC_{50} value of 500 nM. One might conclude that occupation of this space is not absolutely forbidden but definitely hinders the binding to the enzyme.

Returning to the modeling of **19a**, we rationalized that the lack of ACE activity was due to poor overlap along the backbone of the molecule, i.e., occupation of lipophilic sites above and below the plane of the template. Conversely, another way to model the same compound is to constrain the backbone and examine the conformational effect on the functional face of the molecule. A very important structural feature of dual ACE/NEP inhibitory activity is the proper orientation of the amide bond. Since the relative dipole direction of the amide carbonyls for good inhibitors with the active site of ACE and NEP are opposite, some degree of flexibility within the molecule is crucial for dual activity. For the ortho-substituted benzofused macrocycles, steric repulsion between the methylene side chain and the amide carbonyl prevents the amide bond from occupying a favorable conformation required for good ACE interaction. Elimination of the steric interaction between the amide bond and the methylene backbone could be accomplished by replacing the "cis" double bond constrained within the aromatic ring/macrocycle with a "trans" double bond. Preparation of the meta substituted P_1^1 benzo derivatives would satisfy this goal.

The overlap of the meta-substituted benzofused macrocycle **16a** on the ACE template is shown in Figure 7. In contrast to **19a**, the structural overlay of **16a** clearly shows the absence, in the assumed forbidden space, of

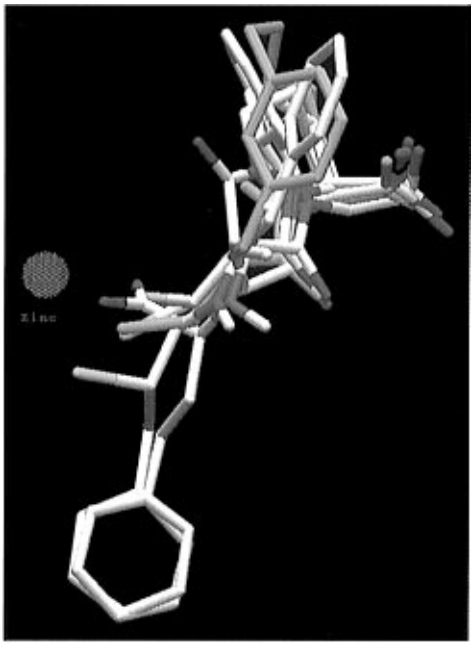

Figure 7. Thirteen-membered ring P_1'(S,S) meta-substituted benzofused macrocyclic lactam **16a** superimposed on the ACE template. Fits well on the template which is consistent with experimental results.

Table 3. *In Vitro* NEP, ACE, and Thermolysin Inhibition of P_1' Meta-Substituted Benzofused Macrocyclic Lactams

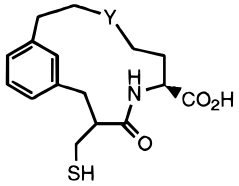

Y = $(CH_2)_n$

			IC_{50} (nM)		
compd	ring size	stereochem	NEP	ACE	TL
14a	14	S	4	175	34000
14b	14	R	445	118	>10000
16a	13	S	8	4	48000
16b	13	R	1000	1400	>10000

the protruding methylene chain. In addition to excellent overlap of the backbone and the functional face of the molecule with the template, a low strain energy is calculated for this conformation. Therefore, good binding to the enzyme would be anticipated. Experimentally, **16a** inhibits ACE with IC_{50} = 4 nM (Table 3).

The (*R,S*) diastereomer (**16b**) when tested as an inhibitor of ACE was found to be considerably less active than the (*S,S*) diastereomer (IC_{50} = 1.4 μM). The results from template fitting shows a small directional change for the carboxyl group and a poor overlap of the methylene sulfhydryl moiety, as well as some twisting out of plane of the methylene backbone chain. These changes from optimal overlap should result in decreased enzyme interactions, as observed.

The 14-membered ring macrocycles in the meta substituted series **14a** and **14b** ((*SS*) and (*RS*) diastereomers) showed moderate ACE inhibition of 187 and 118 nM, respectively. To accommodate the larger ring size, a less than optimal template overlap was observed due to twisting of the aromatic ring out of the template volume. Both structures are predicted to interact with ACE to a lesser degree than **16a** based on template overlay as observed.

Table 4. Energy and Volume Calculations of Host Fit to ACE Template

compd	ACE IC_{50} (nM)	superimposition energy (kJ/mol)[b]	strain energy[c] (kJ/mol)	volume (A^3)[d]	visual description
16a	4	−337	5	458	excellent match
16b	1400	−334	2	457	carbon adjacent to sulfur does not match the template
14a	175	−338	9	467	extends beyond template on top
14b	118	−339	13	464	extends beyond template on top
17a	>10000	−334	31	449	extends beyond template in back
17b	>10000	−332	17	449	extends beyond template in back
18a	8000	−335	39	462	alkane chain extends beyond template near the carboxyl group
18b	2000	−335	19	455	good match
19a	>10000	−333	4	463	extends beyond template in back
19b	>10000	−339	12	465	extends beyond template in back
20 (*S,S*)	*a*	−350	26	474	extends beyond template in back
20 (*S,R*)	*a*	−317	15	480	poor match
20 (*R,S*)	*a*	−331	26	488	extends beyond template in back; sulfur and adjacent carbon do not superimpose
20 (*R,R*)	*a*	−337	46	476	carboxylate and amide carbonyl do not superimpose
21 (*S,S*)	*a*	−347	15	493	good match
21 (*S,R*)	*a*	−336	39	491	carboxylic acid does not match template
21 (*R,S*)	*a*	−342	25	494	good match
21 (*R,R*)	*a*	−329	43	494	sulfur, adjacent methylene, and carboxylic acid do not match template
22 (*S,S*)	*a*	−353	22	491	amide carbonyl does not superimpose
22 (*S,R*)					no conformation found with phenyl ring on the carboxylic acid side of the template
22 (*R,S*)	*a*	−364	23	489	extends slightly beyond template in back
22 (*R,R*)	*a*	−345	25	499	carboxylic acid does not match template

[a] See Table 2 for IC_{50} values. [b] A measure of the match between the host and the template. [c] The difference between the energy of the superimposed conformation and the global minimum internal energy of the host in a vacuum. [d] The volume Å^3 is the sum of the template (433.8) and the non-superimposible volume of the host.

The goal of this research project was to convert our existing NEP inhibitors into dual ACE/NEP inhibitors. As described earlier, we used molecular modeling tools to rationalize why the ortho-substituted macrocycles were potent NEP inhibitors, but devoid of good ACE inhibitory activity. A minor structural change produced the meta-substituted benzofused macrocycles (13- and 14-membered rings) which resulted in dual ACE/NEP activity. The most potent dual inhibitor was **16a**, IC_{50} = 8 nM for NEP and 4 nM for ACE.

The NEP activities of compounds **14a,b** and **16a,b** are shown in Table 3. However, using the molecular modeling program based on thermolysin described in the previous paper, the prediction of NEP inhibitory activity for the meta-substituted derivatives **14a** and **16a** should be minimal. However potent NEP inhibition, IC_{50} = 8 nM and IC_{50} = 4 nM, was observed with compounds **14a** and **16a**, respectively. As predicted the activity against thermolysin was poor (48 and 34 μM, respectively). As pointed out earlier, compounds with different size substituents in the P_1' pocket have dramatic differences in binding affinity to thermolysin and NEP. For example, occupation of the P_1' pocket of NEP by a biphenyl group significantly enhances binding potency in the dicarboxylic acid[31a,b] and aminophosphonic acid series[32] as compared to the unsubstituted phenyl derivatives. Therefore the depth of the P_1' pocket is clearly different between NEP and thermolysin. However, less is known about the width of the NEP P_1'pocket. Examining the area surrounding the P_1' site in the thermolysin model of either **14a** or **16a** (Figure 8) shows the meta substituents protruding from the cavity, unlike the ortho-derived benzofused macrocycle **17a**, shown in the preceding paper. The NEP binding results of **14a** and **16a** could be explained if one assumes NEP is deeper and wider than thermolysin in this region of the enzyme.

The (*R,S*) diastereomers, 13- and 14-membered ring macrocycles, **14b** and **16b,** are considerably weaker as NEP inhibitors than the corresponding (*S,S*) diastereomers, with IC_{50} values of 445 and 1000 nM, respectively. Excluding the effect at the P_1' pocket, visual inspection of **14b** and **16b** in thermolysin show poor interaction of the functional face of the molecules in the thermolysin model. Therefore weaker interactions would be expected.

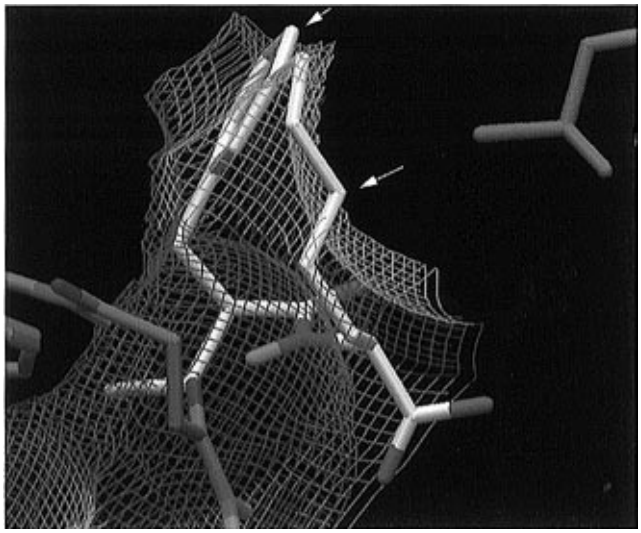

Figure 8. Thirteen-membered ring P_1'(S,S) meta-substituted benzofused macrocyclic lactam **16a** in the active site of thermolysin. Arrows indicate atoms penetrating outside the accessible surface, indicating a poor fit of the macrocycle in the active site.

In summary, the requirements for both ACE and NEP inhibitory activity in the same molecule are good hydrophobic interactions, zinc chelation, carboxylate and hydrogen binding, and flexibility of the amide bond which can occupy two different low-energy conformations. Although conformational restrictions are usually a desirable property, in this case, a constrained amide bond would not allow proper alignment for beneficial hydrogen bonding to occur with both enzymes. This can be appreciated visually in Figures 7 and 8. The ACE

template shows the direction of the amide NH pointing into the ring with the carbonyl moiety exocyclic to the macrocycle cavity. In contrast, the NH of the NEP template is rotated in the opposite direction. A dual inhibitor must be flexible enough to meet both of these requirements. This series of compounds benefit from the rigid nature of the macrocycle structure. However, these compounds demonstrate a balance between rigidity and flexibility enabling the molecules to meet both of the requirements necessary for dual ACE and NEP inhibition.

We have shown, using molecular modeling tools, how inhibitors bind to two similar enzymes, ACE and NEP. We rationalized how small structural changes would allow selective NEP inhibitors to adopt new conformations allowing dual inhibition to occur. These compounds will not be drugs due to their inherent synthetic difficulties of macrolactonization; however, they do represent a good example of how medicinal chemistry and molecular modeling were used to design, refine, and prioritize synthetic targets.

Experimental Section

General procedures. ^{1}H NMR spectra were recorded on Varian XL 400 MHz, Varian VR 300 MHz, and/or Bruker AC 250 MHz spectrometers with tetramethylsilane as internal standard. Infrared spectra were recorded on a Nicolet 5SXFT spectrometer. Optical rotations were measured with a Perkin-Elmer Model 241 polarimeter. Melting points were taken on a Thomas-Hoover melting point apparatus and are uncorrected.

(4*S*)-4-[6-(3-Bromophenyl)-3-hexenyl]-3-*t*-BOC-2,2-dimethyloxazolidine (3). To a mixture of phosphonium salt **2** (37g, 63 mmol) and aldehyde **1** (8.6g, 33.4 mmol) in 500 mL of methylene chloride was added 63 mmol of 1.0 M potassium *tert*-butoxide in THF at 0 °C. Disappearance of starting material was monitored by TLC (2.5 h). To the reaction mixture was added silica gel. The reaction mixture was evaporated to dryness and flash chromatographed on silica gel eluting with ether/hexane (1:4) to give 9.3 g (64%) of **3** as a colorless oil.

3-[6-[4(*S*)-(3-*t*-BOC-2,2-dimethyloxazolidinyl)]-3-hexenyl]-benzaldehyde (4). The aryl bromide **3** (9.3 g, 21.2 mmol) in 200 mL of THF was cooled to −78 °C. A solution of 2.5 M nBuLi (15.3 mL, 38.3 mmol) was added dropwise. After completion of the nBuLi addition, DMF was added and the mixture was warmed to 0 °C over a 1 h period. The reaction solution was poured into ice water and extracted with ether two times. The ethereal layer was washed with water (2×) and brine (2×), dried over $MgSO_4$, filtered, and evaporated to dryness. The residue was flash chromatographed on silica gel, eluting with ether/hexane (1:3), affording 5.16 g (63%) of **4** as a colorless oil: ^{1}H NMR ($CDCl_3$) δ 9.97 (s, 1H), 7.7 (s, 2H), 7.43 (m, 2H), 5.40 (m, 2H), 3.85 (m, 1H), 3.69 (d, 2H), 2.7 (t, 2H), 2.34 (m, 2H), 1.9 (m, 2H), 1.7 (m, 2H), 1.56 (s, 3H), 1.50 (s, 3H), 1.40 (s, 9H).

2-[[3-[6-[4(*S*)-(3-*t*-BOC-2,2-dimethyloxazolidinyl)]-3-hexenyl]phenyl]methylene]-1,3-propanedioic Acid 1-Methyl 3-Benzyl Ester (5). A mixture of benzyl methyl malonate (2.79 mL, 14.6 mmol), piperidine (0.99 mL, 10.0 mmol), benzoic acid (0.93 g, 7.6 mmol), and the aldehyde **4** (5.16 g, 13.3 mmol) in 200 mL of toluene was refluxed with water removal using a Dean−Stark condenser for 6 h. The mixture was cooled to room temperature, stirred overnight, and diluted with ether, and the organic layer was washed with 1 N HCl (2×), $NaHCO_3$ (2×), and brine (2×), dried ($MgSO_4$), and evaporated to dryness. The residue was chromatographed on silica gel eluting with ether/hexane (1:3) to give 6.15 g (82%) of **5** as a yellow oil: ^{1}H NMR ($CDCl_3$) δ 7.75 (d, 1H), 7.4−7.1 (m, 8H), 5.32 (m, 2H), 5.29 (s, 2H), 3.84 (s, 3H), 3.8 (m, 2H), 3.7 (m, 1H), 2.65 (t, 1H), 2.08 (t, 1H), 2.3 (m, 2H), 1.95 (m, 2H), 1.6 (m, 2H), 1.55 (two s, 3H), 1.45 (two s, 9H), 1.25 (s, 3H).

2-[[3-[6-[4(*S*)-(3-t-BOC-2,2-dimethyloxazolidinyl)]hexyl]phenyl]methyl]-1,3-propanoic Acid 1-Methyl Ester (6). A suspension of 10% Pd/C (0.75 g) and diester **5** (6.1 g, 10.9 mmol) in 150 mL of ethyl acetate was hydrogenated at 50 psi for 17 h. The mixture was recharged with hydrogen and shaken for an additional 6 h. The reaction was concentrated and filtered through a pad of Celite. Solvent was removed to give 5.1 g (93%) of **6**. The product was used as is in the next step: ^{1}H NMR ($CDCl_3$) δ 7.17 (t, 1H), 7.0 (s, 1H), 6.98 (d, 2H) 3.86 (m, 1H), 3.70 (s, 3H), 3.70 (m, 2H), 3.20 (d, 2H), 2.55 (t, 2H), 1.53 (s, 3H), 1.50 (s, 3H), 1.40 (s, 9H), 1.3−1.6 (m, 10H).

[[3-(7(*S*)-Amino-8-hydroxyoctyl)phenyl]methyl]-1,3-propanedioic Acid 1-Methyl Ester (7). A solution of **6** (5.0 g, 10.2 mmol) in 30 mL of methylene chloride at 0 °C was purged with dry HCl gas for 5 min. The ice bath was removed, HCl gas was bubbled into the solution for an additional 5 min, and the solution was stirred at room temperature overnight. The solvent was removed, and the residue was used as is in the next step.

(6*S*)-6-(Hydroxymethyl)-4-oxo-5-azabicyclo[11.3.1]-heptadeca-1(17),13,15-triene-3-carboxylic Acid Methyl Ester (8). To a solution of EDCI (3.96 g, 20.4 mmol) and HOBT (2.12 g, 15.7 mmol) in 5 L of methylene chloride was slowly added **7** (3.9 g, 11.1 mmol) in 35 mL of DMF, triethylamine (7.4 g, 10.2 mmol), and 500 mL of methylene chloride. The solution was mixed with a mechanical stirrer overnight. The solvents were removed under reduced pressure and taken up in ethyl acetate and sodium bicarbonate solution. The organic layer was separated. The aqueous layer was re-extracted with ethyl acetate, and the organics were combined, washed with 1 N HCl and brine, dried ($MgSO_4$), filtered, and evaporated to dryness. The residue was chromatographed on silica gel, eluting with ethyl acetate to give 1.3 g (35%) of **8** as a mixture of diastereomers: ^{1}H NMR ($CDCl_3$) δ 7.2−6.9 (m, 4H), 6.78 (d, 0.3H), 5.4 (d, 0.7H), 3.95 (m, 1H), 3,75 (s, 0.3H), 3.72 (s, 0.7H), 3.7−3.1 (m, 5H), 2.6 (m, 1H), 2.1 (m, 1H), 1.7 (m, 1H), 1.4−1.0 (m, 9H).

(6*S*)-4-Oxo-5-azabicyclo[11.3.1]heptadeca-1(17),13,15-triene-3,6-dicarboxylic Acid 3-Methyl Ester (9). The macrocyclic lactam alcohol **8** (1.3 g, 3.9 mmol) in 50 mL of acetonitrile and 50 mL of water was oxidized with sodium periodate (3.34 g, 15.6 mmol) and ruthenium trichloride hydrate (0.019 g, 0.086 mmol). The mixture was stirred for 30 min at room temperature and left standing for 2 h. The reaction mixture was diluted with methylene chloride, and the organic layer was washed with water, dried ($MgSO_4$), filtered, and evaporated to dryness to give 1.13 g of **9** as a crude product. NMR shows (DMSO-d_6) amide protons at δ 8.25 (d, 0.3H), 6.2 (d, 0.7H) and two methyl ester protons at 3.75 (s, 0.3H), 3.70 (s, 0.7H). The compound was used without further purification in the next step.

(6*S*)-4-Oxo-5-azabicyclo[11.3.1]heptadeca-1(17),13,15-triene-3,6-dicarboxylic Acid (10). To the ester acid **9** (1.1g, 3.2 mmol) in 10 mL of THF was added 8.5 mL of 1 N NaOH (2.6 equiv). The reaction mixture was stirred overnight and diluted with ether. The aqueous layer was acidified and re-extracted with ethyl acetate, dried ($MgSO_4$), filtered, and concentrated to dryness to give 1.0 g of diacid **10**. ^{1}H NMR shows two amide protons (DMSO-d_6) δ at 8.27 (d, 0.7H), 8.19 (d, 0.3H). The diacid was used without further purification in the next step.

(6*S*)-3-Methylene-4-oxo-5-azabicyclo[11.3.1]heptadeca-1(17),13,15-triene-3-carboxylic Acid (11). The diacid **10** (1.0 g, 3.1 mmol) was refluxed for 3 h with paraformaldehyde (0.135 g, 4.5 mmol) and piperidine (0.059 mL, 0.60 mmol) in 5 mL of pyridine. The mixture was cooled, concentrated, and taken up in an ethyl acetate/1 N HCl solution. The organic layer was washed with HCl and brine, dried ($MgSO_4$), and concentrated to give 0.9 g (96%) of the exo-methylene product **11**: ^{1}H NMR ($CDCl_3$) δ 7.23 (d, 1H), 7.19 (d, 1H), 7.06 (d, 1H), 7.0 (d, 1H), 6.08 (d, 1H), 5.9 (s, 1H), 5.55 (s, 1H), 4.57 (m, 1H), 3.93 and 3.52 (dd, 2H), 2.64 (m, 2H) 1.8−1.0 (m, 10H).

(6*S*)-3-[(Acetylthio)methyl]-4-oxo-5-azabicyclo[11.3.1]-heptadeca-1(17),13,15-triene-6-carboxylic Acid (12). The exo-methylene macrocyclic lactam **11** (0.9 g, 3.0 mmol) was stirred in thioacetic acid (10 mL) for 2 days, concentrated to give **12**, and used as is in the next step.

3-[(Acetylthio)methyl]-4-oxo-5-azabicyclo[11.3.1]-heptadeca-1(17),13,15-triene-6-carboxylic Acid Methyl

Ester [13a (3*S*,6*S*) Diastereoisomer, 13b (3*R*,6*S*) Diastereoisomer]. To the acid **12** (crude product, 3.0 mmol theoretical) in 10 mL of methanol at 0 °C was added diazomethane in ether. The solution was stirred at room temperature for 30 min, concentrated, and chromatographed on silica gel, eluting with ethyl acetate/hexane (1:4) to give 346 mg of the (*S*,*S*) isomer **13a** and 300 mg of the (*R*,*S*) isomer **13b**. The (*R*,*S*) diastereomer **13b** was crystallized from methylene chloride−hexane−ether to obtain X-ray quality crystals. **13a:** ^{1}H NMR ($CDCl_3$) δ 7.2 (m, 2H), 7.0 (m, 2H), 5.86 (d, 1H), 4.30 (m, 1H), 3.7 (s, 3H), 3.3−2.5 (multiplets, 7H), 2.37 (s, 3H), 1.70−1.0 (m, 10H). **13b:** $[\alpha]_D = +56.9$ ($c = 10.1$ CH_2Cl_2); ^{1}H NMR ($CDCl_3$) δ 7.15 (m, 2H), 7.0 (m, 2H), 5.71 (d, 1H), 4.48 (m, 1H), 3.17 (s, 3H), 3.1 (d, 2H), 2.84 (m, 2H), 2.57 (m, 2H), 2.37 (s, 3H), 1.7−1.0 (m, 10H).

Compounds (3*R*,6*S*)-3-(mercaptomethyl)-4-oxo-5-azabicyclo[10.3.1]hexadeca-1(16),12,14-triene-6-carboxylic acid (15a) and (3*S*,6*S*)-3-(mercaptomethyl)-4-oxo-5-azabicyclo[10.3.1]hexadeca-1(16),12,14-triene-6-carboxylic acid (15b), the 13-membered ring S-acetyl derivatives, were prepared analogous to **13a** and **13b**, starting from the aldehyde **1b** derived from *S*-aspartic acid.

15a: ^{1}H NMR ($CDCl_3$) δ 7.25 (m, 1H), 7.0 (m, 3H), 5.6 (d, 1H), 4.02 (m, 1H), 3.65 (s, 3H), 3.2 (m, 3H), 2.7 (m, 2H), 2.55 (s, 3H), 1.7 (m, 4H), 1.3 (m, 2H), 0.68 (m, 2H). **15b:** ^{1}H NMR ($CDCl_3$) δ 7.2 (m, 1H), 7.0 (m, 3H), 5.40 (d, 1H), 4.5 (m, 1H), 3.66 (s, 3H), 3.2−3.4 (m, 7H), 2.33 (s, 3H), 1.87 (m, 2H), 1.35 (m, 6H).

3-(Mercaptomethyl)-4-oxo-5-azabicyclo[11.3.1]heptadeca-1(17),13,15-triene-6-carboxylic Acid [14a (3*S*,6*S*) Diastereomer, 14b (3*R*,6*S*) Diastereomer]. The thioacetate methyl ester **13a** (200 mg, 0.51 mmol) in 15 mL of THF and 4 mL of water was deoxygenated by purging the solution with nitrogen. To this solution was added lithium hydroxide (85 mg, 2.0 mmol) and stirring was continued for 4 h. The reaction was quenched with 1 N HCl, and the mixture was extracted with ethyl acetate, dried ($MgSO_4$), filtered, and concentrated to give 172 mg (98%) of **14a** as a colorless solid melting at 186−191 °C: ^{1}H NMR (DMSO-d_6) δ 12.3 (br, 1H), 8.02 (d, 1H), 7.12 (m, 1H), 6.96 (m, 2H), 3.7 (m, 1H), 3.0−2.5 (m, 9H), 1.6 (m, 4H), 1.1 (m, 6H). Anal. ($C_{18}H_{25}NO_3S$) C, H, N. **14b** prepared from **13b**: ^{1}H NMR (DMSO-d_6) δ 12.5 (br, 1H), 8.12 (d, 1H), 7.16 (t, 1H), 6.96 (t, 2H), 4.20 (m, 1H), 2.8−2.3 (m, 9H), 1.8−0.8 (m, 10H). Anal. ($C_{18}H_{25}NO_3S$) C, H, N.

Prepared similarly from **15a** and **15b** respectively are **(3*R*,6*S*)-3-[(acetylthio)methyl]-4-oxo-5-azabicyclo[10.3.1]-hexadeca-1(16),12,14-triene-6-carboxylic acid methyl ester (16a):** ^{1}H NMR ($MeOD_4$) δ 7.2 (m, 1H), 7.0 (m, 3H), 3.56 (m, 1H), 2.9 (t, 2H), 2.7−2.5 (m, 4H), 2.0−1.2 (m, 6H), 0.9 (m, 2H). Anal. ($C_{17}H_{23}NO_3S$) C, H, N.

(3*S*,6*S*)-Methyl 3-[(acetylthio)methyl]-4-oxo-5-azabicyclo[10.3.1]hexadeca-1(16),12,14-triene-6-carboxylic acid (16b): ^{1}H NMR ($MeOD_4$) δ 8.0 (d, 1H), 7.2 (m, 1H), 7.0 (m, 3H), 4.3 (m, 1H), 2.9−2.5 (m, 6H), 2.0−0.8 (m, 8H). Anal. ($C_{17}H_{23}NO_3S$) C, H, N.

TFIND and TFIT. Template making and template fitting were performed using a program called QXP (quick explore).[4a,b] This program explores conformations by making Monte Carlo perturbations in torsion space followed by rapid Cartesian minimization. Atoms which are part of a cyclic system receive Cartesian perturbations at the Monte Carlo step. The program has application scripts for template making (TFIND) and for template fitting (TFIT).

For both template applications the program uses an extended force field potential which includes a superposition energy. When the superposition energy is switched on, atoms that are close to each other in space and of similar chemical type but belong to different molecules receive an attractive potential which forces them to superimpose. Atoms are typed according to hydrophobicity, hydrogen bonding character, and formal charge. The internal energies of the aligned molecules are computed with the intermolecular electrostatic and van der Waals forces switched off. These searches result in structures of low internal strain energy which are aligned to optimize the match between atoms.

For template finding, several molecules can be submitted. These molecules are allowed to translate, rotate, and alter their conformations in torsion space. Various conformations of the cyclic parts of the molecules are also generated.

TFIT is used to evaluate superimposition of molecules on a proposed template or pharmacophore. The template is fixed and a single test molecule is fitted to it using superimposition plus internal energy. TFIT explores the fit of different conformations of cyclic molecules by generating a set of low-energy conformations (Monte Carlo search with internal energy minimization) and then fitting all the conformations using torsional, rotational, and transitional degrees of freedom.

The output of TFIT contains a set of conformers which fit the template. The ligand strain energy and the superposition energy are reported for each conformation. The ligand strain energy is the difference between the energy of the superimposed conformation and the global minimum internal energy of the compound in vacuum. The superposition energy is a measure of the match between the test compound and the template. This energy is computed using the superposition potential: when an atom of the ligand approaches an atom of the template of similar type, a negative potential energy is experienced. The superposition energy reaches a minimum value when two atoms of the same type are superimposed. This term is a useful measure for comparing the degree of superimposition that test compounds with closely similar structures can achieve.

Acknowledgment. We thank the CIBA analytical staff in Summit, NJ, for collecting the analytical data. We also thank Ms. C. Berry, Ms.Y. Sakane, Mr. M. Beil, and Ms. T. Gerlock for assistance in *in vitro* measurements of NEP and TLN and the ANP assay. The TFIT and TFIND programs are available from Colin McMartin.

References

(1) (a) Robl, J. A.; Cimarusti, M. P.; Simpkins, L. M.; Brown, B.; Ryono, D. E.; Bird, J. E.; Asaad, M. M.; Schaeffer, T. R.; Trippodo, N. C. Dual Metalloprotease Inhibitors. 6. Incorporation of Bicyclic and Substituted Monocyclic Azepinones as Dipeptide Surrogates in Angiotensin-Converting Enzyme/Neutral Endopeptidase Inhibitors *J. Med. Chem.* **1996**, *39*, 494−502. (b) De Lombaert, S.; Tan, J.; Stamford, L.; Sakane, Y.; Berry, C.; Ghai, R. D. Dual Inhibition of Neutral Endopeptidase and Angiotensin-Converting Enzyme by N-Phosphonomethyl and N-Carboxyalkyl Dipeptides. *Bioorg. Med. Chem. Lett.* **1994**, *4*, 2715−2720. (c) MacPherson, L. J.; Baybert, E. K.; Capparelli, M. P.; Bohacek, R. S.; Clarke, F. H.; Ghai, R. D.; Sakane, Y.; Berry, C. J.; Peppard, J. V.; Trapani, A. Design and Synthesis of an Orally Active Macrocyclic Neutral Endopeptidase 24.11 Inhibitor. *J. Med. Chem.* **1993**, *36*, 3821−3828. (d) Bhagwat, S. S.; Fink, C. A.; Gude, C.; Chan, K.; Qiao, Y.; Sakane, Y.; Berry, C.; Ghai, R. D. 4-Substituted Proline Derivatives that Inhibit Angiotensin Converting Enzyme and Neutral Endopeptidase 24.11. *Bioorg. Med. Chem. Lett.* **1994**, *4*, 2673−2676. (e) Turcaud, S.; Gonzalez, W.; Michel, J.; Roques, B. P.; Fournie-Zaluski, C. Diastereoselective Synthesis of Mixanpril, an Orally Active Dual Inhibitor of Neutral Endopeptidase and Angiotensin Converting Enzyme. *Bioorg. Med. Chem. Lett.* **1995**, *5*, 1893−1898. (f) Slusarchyk, W. A.; Robl, J. A.; Taunk, P. C.; Asaad, M. M.; Bird, J. E.; DiMarco, J.; Pan, Y. Dual Metalloprotease Inhibitors. V. Utilization of Bicyclic Azepinonethiazolidines and Azepinonetetrahydrothiazines in Constrained Peptidomimetics of Mercaptoacyl Dipeptides. *Bioorg. Med. Chem. Lett.* **1995**, *5*, 753−758. (g) Das, J.; Robl, J. A.; Reid, J. A.; Sun, C. Q.; Misra, R. N.; Brown, B. R.; Ryono, D. E.; Asaad, M. M.; Bird, J. E.; Trippodo, N. C.; Pritrillo, E. W.; Karanewsky, D. S. Dual Metalloprotease Inhibitors. IV. Utilization of Thiazepines and Thiazines as Constrained Peptidomimetic Surrogates in Mercaptoacyl Dipeptides. *Bioorg. Med. Chem. Lett.* **1994**, *4*, 2193−2198. (h) Robl, J. A.; Sun, C. Q.; Simpkins, L. M.; Ryono, D. E.; Barrish, J. C.; Karanewski, D. S.; Asaad, M. M.; Schaeffer, T. R.; Trippodo, N. C. Dual Metalloprotease Inhibitors. III. Utilization of Bicyclic and Monocyclic Diazepinone Based Mercaptoacetyls. *Bioorg. Med. Chem. Lett.* **1994**, *4*, 2055−2060. (i) Robl, J. A.; Simpkins, L. M.; Sulsky, R.; Sieber-McMaster, E.; Stevenson, J.; Kelly, Y. F.; Sun, C. Q.; Misra, R. N.; Ryono, D. E.; Asaad, M. M.; Bird, J. E.; Trippodo, N. C.; Karanewsky, D. S. Dual Metalloprotease Inhibitors II. Effect of Substitution and Stereochemistry Benzazepinone Based Mercaptoacetyls. *Bioorg. Med. Chem. Lett.* **1994**, *4*, 1795−1800. (j) Robl, J. A.; Simpkins, L. M.; Stevenson, J.; Kelly, Y. F.; Sun, C. Q.; Murugesan, N.; Barrish, J. C.; Asaad, M. M.; Bird, J. E.; Schaeffer, T. R.; Trippodo, N. C.; Petrillo, E. W.; Karanewsky, D. S. Dual Metalloprotease Inhibitors I.

Constrained Peptidomimetics of Mercaptoacyl Dipeptides. *Bioorg. Med. Chem. Lett.* **1994**, *4*, 1789−1794. (k) Delaney, N. G.; Barrish, J. C.; Neubeck, R.; Natarajan, S.; Cohen, M.; Rovnyak, G. C.; Huber, G.; Murugesan, N.; Girotra, R.; Sieber-McMaster, E.; Robl, J. A.; Asaad, M. M.; Cheung, H. S.; Bird, J. E.; Waldron, T.; Petrillo, E. W. Mercaptoacyl Dipeptides as Dual Inhibitors of Angiotensin Converting Enzyme and Neutral Endopeptidase. Preliminary Structure-Activity Studies. *Bioorg. Med. Chem. Lett.* **1994**, *4*, 1783−1788. (l) Gomez-Monterrey, I.; Beaumont, A.; Nemecek, P.; Roques, B. P.; Fournie-Zaluski, M. C. New Thiol Inhibitors of Neutral Endopeptidase EC 3.4.24.11: Synthesis and Enzyme Active Site Recognition. *J. Med. Chem.* **1994**, *37*, 1865−1873. (m) Fournie-Zaluski, M. C.; Coric, P.; Turcaud, S.; Rousselet, N.; Gonzalez, W.; Barbe, P.; Pham, I.; Jullian, N.; Michel, J.; Roques, B. P. New Dual Inhibitor of Neutral Endopeptidase and Angiotensin Converting Enzyme: Rational Design, Bioavailability, and Pharmacological Response in Experimental Hypertension. *J. Med. Chem.* **1994**, *37*, 1070−1083. (n) Stanton, J. L.; Sperbeck, D. M.; Trapani, A. J.; Cote, D.; Sakane, Y.; Berry, C. J.; Ghai, R. D. Heterocyclic Lactam Derivatives as Dual Angiotensin Converting Enzyme and Neutral Endopeptidase 24.11 Inhibitors. *J. Med. Chem.* **1993**, *36*, 3829−3833. (o) Flynn, G. A.; Beight, D. W.; Mehdi, S.; Koehl, J. R.; Giroux, E. L.; French, J. F.; Hake, P. W.; Dage, R. C. Application of a Conformationally Restricted Phe-Leu Dipeptide Mimetic to the Design of a Combined Inhibitor of Angiotensin-I Converting Enzyme and Neutral Endopeptidase 24.11 *J. Med. Chem.* **1993**, *36*, 2420-2423. (p) Bhagwat, S. S.; Fink, C. A.; Gude, C.; Chan, K.; Qiao, Y.; Sakane, Y.; Berry, C.; Ghai, R. D. α-Mercaptoacyl Dipeptides that Inhibit Angiotensin Converting Enzyme and Neutral Endopeptidase 24.11. *Bioorg. Med. Chem. Lett.* **1995**, *5*, 735−738. (q) Fink, C. A.; Qiao, Y.; Berry, C. J.; Sakane, Y.; Ghai, R. D.; Trapani, A. New α-Thiol Dipeptide Dual Inhibitors of Angiotensin-I Converting Enzyme and Neutral Endopeptidase EC 3.4.24.11. *J. Med. Chem.* **1995**, *38*, 5023−5030.

(2) Bohacek, R.; De Lombaert, S.; McMartin, C.; Priestle, J.; Gruetter, M. Three-Dimensional Models of ACE and NEP Inhibitors and their Use in the Design of Potent Duel ACE/NEP Inhibitors .*J. Am. Chem. Soc.* **1996**, *118*, 8231−8249.

(3) Hausin, R. J.; Codding, P. W. Crystallographic Studies of Angiotensin Converting Enzyme Inhibitors and Analysis of Preferred Zinc Coordination Geometry. *J. Med. Chem.* **1990,** *33*, 1940−1947.

(4) (a)McMartin, C.; Bohacek, R. Flexible Matching of Test Ligands to a 3-D Pharmacophore Using a Molecular Superposition Force Field: Comparison of Predicted and Experimental Conformations of Inhibitors of Three Enzymes. *J. Comput. Aided Mol. Des.* **1995**, *9*, 237−250. (b) McMartin, C.; Bohacek, R. QXP; a basic set of powerful, user friendly computer routines for structue-based drug design. *J. Comput.-Aided Mol. Des.*, in press.

(5) Andrews, P. R.; Carson, J. M.; Caselli, A.; Spark, M. J.; Woods, R. Conformational Analysis and Active Site Modelling of Angiotensin-Converting Enzyme Inhibitors. *J. Med. Chem.* **1985,** *28*, 393−399.

(6) Mayer, D.; Naylor, C. B.; Motoc, I.; Marshall, G. R. A Unique Geometry of the Active Site of Angiotensin-Converting Enzyme Consistent with Structure-Activity Studies. *J. Comput.-Aided Mol. Des.* **1987**, *1*, 3−16.

(7) Soubrier, F.; Alhenc-Gelas, F.; Hubert, C.; Allegrini, J.; John, M.; Tregear, G.; Corvol, P. Two putative active centers in human angiotensin I-converting enzyme revealed by molecular cloning. *Proc. Natl. Acad. Sci. U.S.A.* **1988**, *85*, 9386−9390.

(8) Kester, W. R.; Matthews, B. W. Crystallographic Study of the Binding of Dipeptide Inhibitors to Thermolysin: Implications for the Mechanism of Catalysis. *Biochemistry* **1977**, *16*, 2506−2516.

(9) Devault, A.; Lazure, C.; Nault, C.; Seidah, N. g.; Chretien, M.; Kahn, P.; Powell, J.; Mallet, J.; Beaumont, A.; Roques, B. P.; Crine, P.; Boileau, G. Amino Acid sequence of rabbit kidney neutral endopeptidase 24.11 (enkephalinase) deduced from a complementary DNA. *EMBO J.* **1987**, *6*, 1317−13422.

(10) Vallee, B. L.; Auld, D. S. Zinc Coordination, Function, and Structure of Zinc Enzymes and Other Proteins. *Biochemistry* **1990**, *29*, 5647−5659.

(11) Jongeneel, C. V.; Bouvier, J.; Bairoch, A. A unique signature identifies a family of zinc-dependent metallopeptidases. *FEBS Lett.* **1989**, *242*, 211−214.

(12) Stoeckler, W.; Grams, F.; Baumann, U.; Reinemer, P.; Gomix-Rueth, F.; McKay, D. B.; Bode, W. The metzincins - Topological and sequential relations between the astacins, adamalysisn, serralysins and matrixins(collagenases) define a superfamily of zinc-peptidases. *Protein Sci.* **1995**, *4*, 823−840.

(13) Matthews, B. W. Structural Basis of the Action of Thermolysin and Related Zinc Peptidases. *Acc. Chem. Res.* **1988**, *21*, 333−340.

(14) Bode, W.; Gomis-Rueth, F.-X.; Huber, R.; Zwilling, R.; Stoeckler, W. Structure of astacin and implications for activation of astacins and zinc-ligation of collagenases. *Nature* **1992**, *358*, 164−167.

(15) Lovejoy, B.; Cleasby, A.; Hassell, A. M.; Longley, K.; Luther, M. A.; Weigl, D.; McGeehan, G.; McElroy, A. B.; Drewry, D.; Lambert, M. H.; Jordan, S. R. Structure of the Catalytic Domain of Fibroblast Collagenase Complexed with an Inhibitor. *Science* **1994**, *263*, 375−377.

(16) Gooley, P. R.; O'Connell, J. F.; Marcy, A. I.; Cuca, G. C.; Salowe, S. P.; Bush, B. L.; Hermes, J. D.; Esser, C. K.; Hagmann, W. K.; Springer, J. P.; Johnson, B. A. The NMR Structure of the Inhibited Catalytic Domain of Human Stromelysin-1. *Struct. Biol.* **1994**, *1*, 111−118.

(17) Borkakoti, N.; Winkler, F. K.; Williams, D. H.; D'Arcy, A.; Broadhurst, M. J.; Brown, P. A.; Johnson, W. H.; Murray, E. J. Structure of the catalytic domain of human fibroblast collagenase complexed with an inhibitor. *Struct. Biol.* **1994**, *1*, 106−110.

(18) Bode, W.; Reinemer, P.; Huber, R.; Kleine, T.; Schnierer, S.; Tschesche, H. The X-ray crystal structure of the catalytic domain of human neutrophil collagenase inhibited by a substrate analogue reveals the essentials for catalysis and specificity. *EMBO J.* **1994**, *13*, 1263−1269.

(19) Stams, T.; Spurlino, J. C.; Smith, D. L.; Wahl, R. C.; Ho, T. F.; Qoronfleh, M. W.; Banks, T. M.; Rubin, B. Structure of human neutrophil collagenase reveals large S1′ specificity pocket. *Struct. Biol.* **1994,** *1*, 119−123.

(20) Becker, J. W.; Marcy, A. I.; Rokosz, L. L.; Axel, M. G.; Burbaum, J. J.; Fitzgerald, P. M. D.; Cameron, P. M.; Esser, C. K.; Hagmann, W. K.; Hermes, J. D.; Springer, J. P. Stromelysin-1: Three-dimension structure of the inhibited catalytic domain and the C-truncated proenzyme. *Protein Sci.* **1995**, *4*, 1966−1976.

(21) Browner, M.; Smith, W.; Castelhano, A. Matrilysin-Inhibitor complexes: common themes among metalloproteases. *Biochemistry* **1995**, *34*, 660−6610.

(22) Gomis-Rueth, F. X.; Kress, L. F.; Kellermann, J.; Mayr, I.; Lee, X.; Huber, R.; Bode, W. Refined 2.0 A^0 X-ray crystal Structure of the Snake Venom Zinc-endopeptidase Adamalysin II. *J. Mol. Biol.* **1994**, *239*, 513−544.

(23) Baumann, U.; Wu, S.; Flaherty, K. M.; McKay, D. B. Three-dimensional X-ray crystallographic structure of the alkaline protease of *Pseudomonas aeruginosa*. *EMBO J.* **1993**, *12*, 3357−3364.

(24) Bode, W.; Gomis-Rueth, F.-X.; Stoeckler, W. Astacins, serralysins, snake venom and matrix metalloproteinases exhibt identical zinc-binding environments (HEXXHXXGXXH and Met-trun) and topologies and should be grouped into a common family, the "metzincins". *FEBS* **1993**, *331*, 134−140.

(25) Devault, A.; Sales, N.; Nault, C.; Beaumont, A.; Roques, B. P.; Crine, P.; Boileau, G. Exploration of the catalytic site of endopeptidase 24.11 by site-directged mutagenesis. Histidine residues 583 and 587 are essential for catalysis. *FEBS Lett.* **1988**, *231*, 54−58.

(26) Devault, A.; Nault, C.; Zollinger, M.; Fournie-Zaluski, M. C.; Roques, B. P.; Crine, P.; Boileau, G. Expression of neutral endopeptidase (enkephalinase) in heterologous COS-1 cells. *J. Biol. Chem.* **1988**, *263*, 4033−4040.

(27) Williams, T. A.; Corvol, P.; Soubrier, F. Identification of Two Active Site Residues in Human Angiotensin I-Converting Enzyme. *J. Biol. Chem.* **1994**, *269*, 29430−29434.

(28) Moual, H. L.; Devault, A.; Roques, B. P.; Crine, P.; Boileau, G. Identification of Glutamic Acid-646 as a Zinc-coordinating Residue in Endopeptidase-24.11. *J. Biol. Chem.* **1991**, *266*, 15670−15674.

(29) Flynn, G. A.; Beight, D. W.; Mehdi, S.; Koelh, J. R.; Giroux, E. L.; French, J. F.; Hake, P. W.; Dage, R. C. Application of a Conformationally Restricted Dipeptide Mimetic to the Design of a Combined Inhibitor of Angiotensin I-Converting Enzyme and Neutral Endopeptidase 24.11. *J. Med. Chem.* **1993**, *36*, 2420−1423.

(30) Mohamadi, F.; Richards, N. G. J.; Guida, W. C.; Liskamp, R.; Lipton, M.; G., C.; Chang, G.; Hendirckson, T.; Still, W. C. MACROMODEL - An Integrated Software System for Modelling Organic and Bioorganic Molecules Using Molecular Mechanics. *J. Comput. Chem.* **1990**, *11*, 440−467.

(31) (a)Berger, J. G. A Novel Approach to Analgesia: Synthesis and Structure-Activity Relationships of Some Potent and Selective Inhibitors of Enkephalinase. In *Abstracts of the 19th National Medicinal Chemistry Symposium*; Tucson, AZ, June 17−21, ***1984***; pp 39−52. (b) Ksander, G. M.; Ghai, R. D.; de Jesus, R.; Diefenbacher, C.; Yuan, A.; Berry, C.; Sakane,Y.; Trapani, A. Dicarboxylic Acid Dipeptide Neutral Endopeptidase Inhibitors. *J. Med. Chem.* **1995**, *38*, 1689−1700.

(32) De Lombaert, S.; Erion, M. E.; Tan, J.; Blanchard, L.; El-Chehabi, L.; Ghai, R. D.; Sakane, Y.; Berry, C.; Trapani, A. N-Phosphonomethyl Dipeptides and Their Phosphonate Prodrugs, a New Generation of Neutral Endopeptidase (NEP, EC 3.4.24.11) Inhibitors. *J. Med. Chem.* **1994**, *37*, 498−511.

JM960583G